

Highly sensitive and high throughput magnetic resonance thermometry using superparamagnetic nanoparticles

Darshan Chalise^{1,2*}, David G. Cahill^{1,2,3}

¹*Department of Physics, University of Illinois at Urbana-Champaign, Urbana, IL, 61801, USA*

²*Materials Research Laboratory, University of Illinois at Urbana-Champaign, Urbana, IL, 61801, USA*

³*Materials Science and Engineering, University of Illinois at Urbana-Champaign, Urbana, IL, 61801, USA*

*Corresponding Author – darshan2@illinois.edu

Abstract

Magnetic resonance imaging (MRI) enables non-invasive 3D thermometry during thermal ablation of cancerous tumors. While T_1 or T_2 contrast MRI are relatively insensitive to temperature, techniques with greater temperature sensitivity such as chemical shift or diffusion imaging suffer from motional artifacts and long scan times. We describe an approach for highly sensitive and high throughput MR thermometry that is not susceptible to motional artifacts. We use superparamagnetic iron oxide nanoparticles (SPIONs) to spoil T_2 of water protons. Motional narrowing results in proportionality between T_2 and the diffusion constant, dependent only on the temperature in a specific environment. Our results show, for pure water, the nuclear magnetic resonance (NMR) linewidth and T_2 follow the same temperature dependence as the self-diffusion constant of water. Thus, a T_2 mapping is a diffusion mapping in the presence of SPIONs, and T_2 is a thermometer. For pure water, a T_2 mapping of a 32 x 32 image (voxel size = 1 mm x 1 mm x 3 mm) in a 9.4 T MRI scanner resulted in a temperature resolution of 0.5 K for a scan time of 2 minutes. This indicates a highly sensitive and high throughput MR thermometry technique potentially useful for monitoring of biological tissues during thermal therapies or for diagnosis.

Introduction

Temperature monitoring in biological systems is important during thermal ablation of cancerous tissues to ensure effective treatment and prevent collateral damage of healthy tissues [1]. Temperature is also an indicator of physiological processes [2], and therefore, accurate determination of temperature can be used for diagnosis of diseases.

Due to its ability to obtain non-invasive 3D images, MRI has been routinely used for temperature monitoring during thermal therapies. Current MRI thermometry often utilizes the temperature dependence of the spin-lattice relaxation time (T_1) of water protons [1]. T_1 , sensitive to temperature as it depends on the diffusion of water molecules[3]. While the translational diffusion in water is highly sensitive to temperature (1% change in temperature corresponds to

a 4% change in the diffusion constant at room temperature), the rotational diffusion is not temperature sensitive [3]. A 1% change in temperature typically corresponds to a 3% change in T_1 [1], [3]. Due to intrinsically long acquisition times used in T_1 sequences (Inversion recovery or Saturation recovery), a reasonable acquisition time often results in a temperature resolution of >1.5 K [4]. In many biological systems water T_2 is often limited by T_1 (due to fast diffusion) and therefore, T_2 imaging is also not a sensitive means of thermometry [1].

A highly sensitive MR temperature imaging is performed with proton resonance frequency (PRF) shift imaging or chemical shift imaging (CSI) [5]. The chemical shift of water protons changes by ~ 0.01 ppm/K for water in most tissues, and since the linewidth of water protons is very narrow, a temperature resolution of ~ 0.5 K can be achieved with chemical shift imaging [5]. However, chemical shift imaging is extremely time consuming as the image is entirely phase encoded [1]; a 32×32 image typically takes 32 times more scan time than a T_1 or T_2 imaging. More importantly, the need to obtain a baseline image for phase contrast means that motion in between two images causes significant artifacts [1].

For pure water, at around room temperature, the translational diffusion (D) is also highly temperature dependent due to the high temperature dependence of the hydrogen bonding in water [5]. The sensitivity coefficient, which describes the percentage change in the diffusion constant to one percent change in temperature is about 4 [6]. The sensitivity coefficient is similar for water protons in different tissues [7][8][9], and therefore a (translational) diffusion imaging can be a sensitive thermometer.

However, a diffusion mapping requires a long acquisition time and suffers from interscan gradient instabilities [3]. Even more significantly, similar to CSI, a diffusion mapped MRI image is susceptible to interscan motional artifact [3]. This restricts the application of diffusion mapping for thermometry in living systems.

Apart from MR thermometry using the intrinsic properties of water protons (relaxation times, diffusion constant or chemical shift), various thermometry techniques have been suggested utilizing MR contrast agents. Among these, different phase change contrast agents have been proposed as thermometers [1]. However, the phase change contrast agents only provide a semi-quantitative means of thermometry. Some recent thermometry techniques utilizing contrast agents includes contrast agent inducing large temperature dependence of chemical shifts (1 ppm/K) [10] or field inhomogeneities (or equivalently T_2^*) [11]. While CSI is limited in practical application due to long scan times and motional artifact, T_2^* imaging utilizing the temperature dependence of magnetization is limited in temperature range and susceptible to external field inhomogeneities.

Superparamagnetic iron-oxide nanoparticles (SPIONs) (see [12] for their synthesis and biomedical applications) are routinely used in biological systems for targeted drug delivery [13], MR T_1/T_2 contrast [14] and magnetic particle imaging [15]. In this paper, we demonstrate a

highly sensitive temperature method utilizing SPIONs as T_2 contrast agents, in which we image diffusion as a form of T_2 contrast.

The strong magnetization of the superparamagnetic particles introduces field inhomogeneities and increases the transverse relaxation rate, R_2 , in a liquid [16] [17], i.e.

$$R_2 = R_{2,0} + R_{2,S},$$

Here, $R_{2,0}$ is the relaxation rate in a liquid in the absence of the SPIONs and $R_{2,S}$ is the relaxation rate due to the SPIONs.

As long as the correlation time of the protons hopping through an SPION, $\tau_c (= \frac{d^2}{4D})$, where, 'd' is the diameter of a SPION and D is the translational diffusion constant of proton in the liquid), is smaller than the reciprocal of the resonance frequency shift corresponding to the field inhomogeneity induced by the SPION (i.e. $\Delta\omega \cdot \tau_c \leq 1$), motional narrowing can take place. When motional narrowing takes place, the relaxation induced by SPIONs can be estimated by outer sphere theory of the relaxation of protons in the presence of paramagnetic impurities [16][18] [17][19]:

$$R_{2,S} = \frac{1}{T_2^*} = \frac{5}{9} v_f \tau_c (\Delta\omega)^2$$

Here, v_f is the volume fraction of the SPIONs in the liquid and ' τ_c ' is the correlation time a proton takes to travel across a SPION. $\Delta\omega$ is the average frequency shift of the proton on the surface of the SPION and is given by:

$$\Delta\omega = \sqrt{\frac{4}{5} \frac{\gamma \mu_0 M_s}{3}}.$$

Here, $\gamma = 267.52$ Mrad/T is the gyromagnetic ratio of the proton, μ_0 is the permeability of free space and M_s is the saturation magnetization of a SPION. Our NMR measurements (see results) showed that the outer sphere theory works extremely well (within a factor of 1.2), and the above expression for $R_{2,S}$ is a precise estimate of the relaxation due to SPIONs.

As long as the relaxation induced by SPIONs is much greater than the natural relaxation rate of a proton in a liquid, i.e. $R_2 = R_{2,0} + R_{2,SPION} \approx R_{2,SPION}$, and a T_2 experiment satisfies $\tau_c \ll T_{echo}$, echo pulses are unable to recover the relaxation of proton due to SPIONs [17], and

$$\frac{1}{T_2} = \frac{1}{T_2^*} = R_{2,S} = av_f \tau_c (\Delta\omega)^2 = av_f \frac{d^2}{4D} \left(\frac{\gamma \mu_0 M}{2\pi \cdot 3} \right)^2.$$

Therefore, in the motional narrowing regime, as long as the magnetization of the SPIONs remain constant, and $T_{echo} \gg \tau_c$, proton T_2 in the presence of SPIONs scales linearly with the diffusion constant 'D', and a T_2 contrast imaging is essentially a diffusion contrast imaging.

Since T_2 contrast imaging is significantly faster compared to a conventional diffusion or PRF shift imaging, the method of imaging temperature as a form of T_2 contrast is high throughput. More importantly, T_2 contrast or mapping does not require a baseline image, making this method of thermometry less susceptible to interscan motional artifacts compared to diffusion mapping or chemical shift mapping.

The non-toxicity of superparamagnetic nanoparticles across various tissues (results in [20] show almost no cytotoxicity in most cells up to a SPION volume fraction of 20 ppm), and the strong temperature dependence of water in tissues [7], [9], makes this thermometry potentially utilizable in several biological applications.

Results

Characterization of superparamagnetic iron oxide nanoparticles using SQUID magnetometry

Iron (II, III) oxide nanoparticles (average particle size of 15 nm) suspended in water (5 mg/ml) were purchased from Sigma Aldrich (Product: 900043-5ML). SQUID magnetometry was performed to confirm superparamagnetic behavior and assure there was no clustering of the nanoparticles.

SQUID measurements performed at a field sweep of -0.3 T to 0.3 T at 300K showed a saturation magnetization of 57 emu/g (assuming a Fe_3O_4 concentration of 5 mg/ml in water) at a field of 0.3 T (figure S1a). The results are consistent with the superparamagnetic behavior of the iron oxide nanoparticles [21], as no hysteresis is observed. The superparamagnetic behavior assures there is no clumping of the particles. The results show that the saturation of the magnetization occurs at a field of < 0.3 T, and therefore, for fields used in the NMR and MRI experiments (14.1 T and 9 T respectively), a saturation magnetization (M_s) of 57 emu/g ($= 2.94 \times 10^5$ A/m, assuming the density of $Fe_3O_4 = 5.17$ g/cm³) has been used in comparing the theoretical relaxation rates (Section I) with the experimental results.

Since the Curie temperature of Iron (II, III) oxide is 850 K [22], and the saturation occurs at a field of < 0.25 T, we expect the magnetization of the particles to be independent of temperature in strong magnetic fields typical of a MRI instrument in the range of temperature we are interested in (0° C-100° C). A temperature dependent SQUID measurement (figure S1b) at 0.3 T confirms this. Therefore, any changes in T_2/T_2^* of protons in water can only be attributed to change in the diffusion constant and not the saturation magnetization of the superparamagnetic particles.

NMR linewidth and T_2 measurements

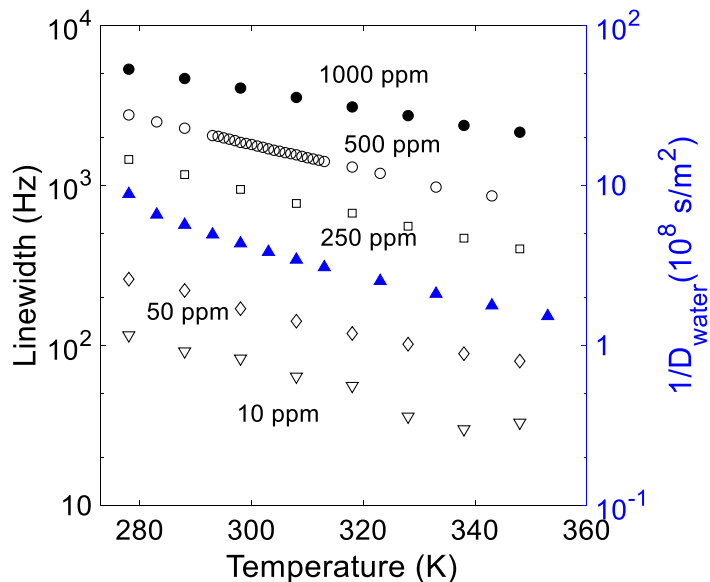
NMR measurements were performed on a 14.1 T Varian Unity/Inova NMR spectrometer to confirm temperature dependent motional narrowing. Temperature dependent linewidth

measurements showed a decrease in NMR linewidth of water protons with increasing temperature, coinciding very closely with the increase in self-diffusion constant of water with temperature (except at very low temperatures where $\Delta\omega \cdot \tau_c \sim 1$, and motional narrowing is not effective). Figure 1 shows the linewidth of water protons for various temperatures and various concentrations of the superparamagnetic nanoparticles. We can see from the figure that the NMR linewidth scales linearly with the concentration of the particle, but the relative change in the linewidth of the protons is independent of the concentration, and is only a function of temperature and scales with the diffusion constant of water (taken from published values in [6]).

At very low concentrations (≤ 65 ppm in our measurement) and at high temperatures, the natural linewidth of water due to imperfect shimming becomes comparable to the linewidth induced by the presence of nanoparticles, and then the decrease in linewidth with temperature deviates from the increase in diffusion constant. This is the lower limit for the concentration of the nanoparticles in our method for linewidth to be a thermometer – the linewidth induced by the particles should be significantly higher compared to the natural proton linewidth in the tissue. The results from the linewidth ($\Delta\nu$) measurements show that a T_2^* ($= \frac{1}{\pi(\Delta\nu)}$) contrast MRI imaging is a diffusion contrast MRI imaging in the presence of superparamagnetic nanoparticles as long as shimming imperfections do not dominate.

When $T_{echo} \gg \tau_c = \frac{d^2}{4D}$, in the absence of external field inhomogeneities, T_2 is equivalent to T_2^* [17], and therefore, a T_2 contrast imaging also is a diffusion contrast imaging. In order to establish the equivalence of T_2 and T_2^* in the presence of the nanoparticles, T_2^* and T_2 measurements ($T_{Echo} = 0.1$ ms) were taken for 3 different concentrations of nanoparticles in water, and the results are included in Figure 2. The results show T_2 and T_2^* are equivalent as long as the linewidth induced due to the nanoparticle is much greater than the natural linewidth of water due to improper shimming. At very low concentrations of nanoparticles and at high temperatures (65 ppm in NMR and 10 ppm in MRI), T_2 still remains a good thermometer, showing the same dependence to the diffusion constant, while T_2^* gets overwhelmed by shimming imperfections.

a)



b)

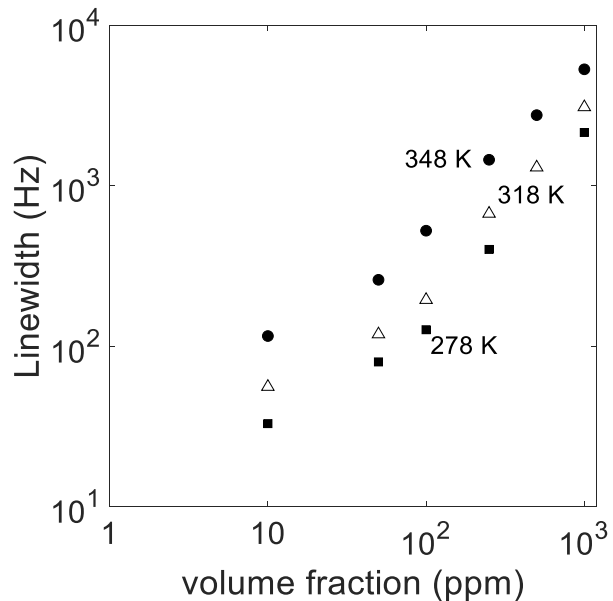


Figure 1. (a) The temperature dependence of NMR linewidths (and consequently T_2^*) of protons in water in the presence of SPIONs and its comparison to the temperature dependence of the diffusion coefficient of proton in water (blue triangles). The linewidths shows the same temperature dependence as the reciprocal of the diffusion constant, until the concentration of the nanoparticles is low and the linewidth due to improper shimming becomes significant (at around

50 ppm nanoparticles by volume). (b) Comparison of NMR linewidth of protons in water with the volume fraction of SPIOs at 278 K (black squares), 318 K (open black triangles) and 348 K (black circles). The linewidths scale linearly with the volume fraction at all temperatures except for low volume fraction where shimming imperfections contribute significantly to the linewidth.

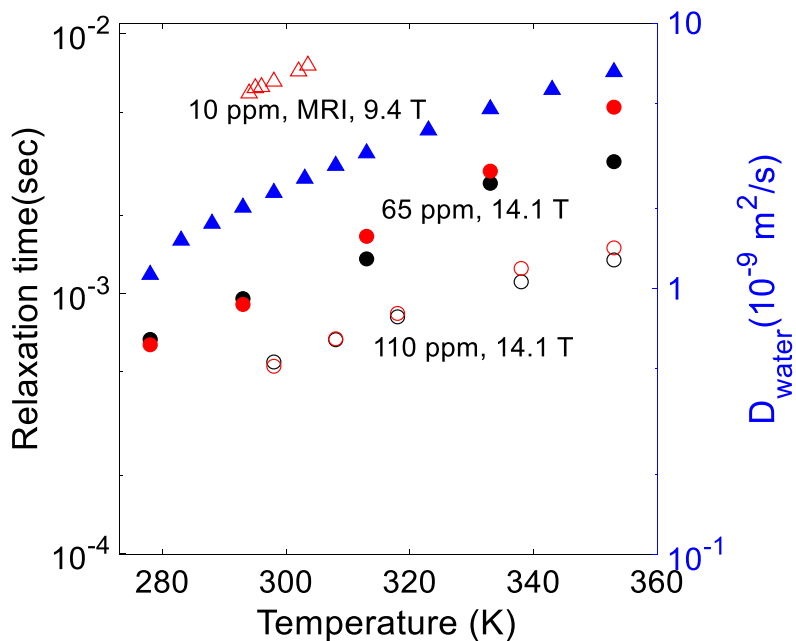


Figure 2. Temperature dependence of relaxation times T_2 (red) and T_2^* (black) at SPION volume fractions of 110 ppm (open circles), 65 ppm (filled circles) and 10 ppm (open triangles). The temperature dependence of the relaxation times are compared with the temperature dependence of the diffusion constant in water (blue filled triangles). The measurements of relaxation times for SPION volume fractions of 110 ppm and 65 ppm were carried out in a Unity/Inova 14.1 T NMR spectrometer while the measurements for the volume fraction of 10 ppm was carried out in Bruker BioSpec 9.4 T preclinical MRI scanner. For lower volume fractions (<65 ppm) and high temperature, T_2^* has a significant contribution from field inhomogeneities due to imperfect shimming while T_2 is not affected and remains a good thermometer.

T_2 contrast MRI

The applicability of the method was demonstrated in pure water (iron oxide nanoparticles present in 10 ppm by volume) on a 9.4 T Bruker BioSpec preclinical MRI system. Isothermal T_2 mapping were performed using multispin multiecho (MSME) sequence [23] at various temperatures in the range $21^\circ\text{C} - 31^\circ\text{C}$. The isothermal T_2 measurements showed an average T_2 variation of about 0.7 % for a specific temperature. Given the sensitivity of ~ 4 at room temperature, this variation in T_2 corresponds to a temperature resolution of about 0.5 K.

Figure 3 shows the increase in average T_2 with increasing temperature (specific values of T_2 vs temperature are included in Figure 2). As expected from the NMR measurements (see Figure 2), the increased in T_2 corresponds to the increase in the self-diffusion constant of water, even for a concentration as small as 10 ppm in pure water.

If no external field inhomogeneities were present, a T_2^* mapping should have been an equivalent thermometry. However, due to the small concentration of nanoparticles used in the MRI measurement and due to the inability to perform a good shimming due to the particles, the external field inhomogeneities were significant enough to cause a larger variation of T_2^* . Therefore, T_2^* mapping had a significantly worse temperature resolution. This also accentuates the fact that our method utilizing the motional narrowing on T_2^* is a more reliable thermometry compared to T_2^* methods utilizing the temperature dependent magnetization of the contrast agents.

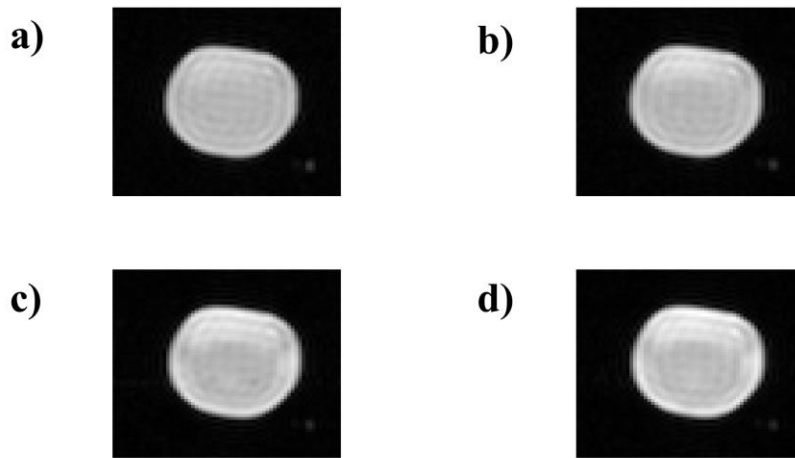


Figure 3. T_2 contrast cross sectional (coronal) images of water in a cylindrical container at 23 °C, 25 °C, 29 °C and 31 °C in the presence of SPIONs (10 ppm by volume). The images are taken with an echo time (T_{Echo}) of 11.2 ms and are the second images at each temperature in a series of MSME images with equal echo spacing of 5.6 ms. The average intensity of the 4th image (at 31°C) is 20% brighter than the average intensity of the 1st image (at 23°C), and the image intensities are consistent with the respective T_2 values of 6.25 ms and 7.56 ms determined from MSME.

Discussion

Our results show, in the presence of superparamagnetic nanoparticles, in the motional narrowing regime, a T_2 contrast imaging/ T_2 mapping is a diffusion contrast imaging/diffusion mapping. However, since T_2 imaging does not require any interscan baseline image, it is not susceptible to motional artifact unlike conventional diffusion imaging. Additionally, since T_2 mapping and especially T_2 contrast imaging is intrinsically faster than diffusion contrast imaging. Therefore, T_2 imaging provides a high resolution thermometry which is also high throughput.

One requirement for this method to be applicable is that the correlation time of protons hopping through an SPION needs to be smaller than the reciprocal of frequency shift induced by the SPION: i.e. $\Delta\omega \cdot \tau_c \leq 1$ (i.e. motional narrowing needs to take place). For the particles used in the experiment ($M_s = 2.94 \times 10^5$ A/m and $d = 15$ nm), $\Delta\omega = 2.9 \times 10^7$ s⁻¹, and in pure water $\tau_c = 2.2 \times 10^{-8}$ s at room temperature ($D = 2.5 \times 10^{-9}$ m²/s). Therefore, the condition of motional narrowing is satisfied. This condition would also be barely satisfied in the extracellular water in blood where the diffusion constant is 40% smaller and consequently the correlation time is 40% larger for the same size of nanoparticles [9]. The condition is, however, not satisfied for intracellular water typically having a diffusion coefficient of $\sim 8 \times 10^{-10}$ m²/s [9]. Therefore, for intracellular water, particles with smaller diameter ($d = 8.5$ nm for $\tau_c = 2.2 \times 10^{-8}$ s) are required for the applicability of the method. This requirement is not difficult to satisfy as SPIONs with diameters ~ 5 nm have been synthesized [18].

The other two requirements for this method to be generally applicable to fluids in tissues are that the superparamagnetic particles significantly spoil the T_2 (i.e. $T_{2,S} \ll T_{2,0}$) and the echo pulses are not able to recover the relaxation due to the SPIONs (i.e. $\tau_c \ll T_{\text{echo}} \sim T_{2, \text{SPION}}$). Even for fluids with T_2 as small as 50 ms (which is less than T_2 values of protons in most tissues [24]), a $T_{2,S}$ of ~ 10 ms can be obtained with a SPION volume fraction of ~ 10 ppm, which is a safe quantity for medical applications [20]. Therefore, the first of these requirements is easily satisfied. Even for a very small T_{echo} of 10 ms, which would be required for fluids with a small $T_{2,S}$ of ~ 10 ms, the typical correlation time is $\sim 10^{-8}$ s, so the second condition is also easily satisfied. Therefore, with a careful selection of SPOIN size and volume fraction, our method can be generally applied to water in tissues and blood.

In vivo application, however, will be challenging due to different values and temperature dependence of the self-diffusion constant of water in different tissues. This is, however, a general challenge in MR thermometry [1] and is not unique to our method.

Finally, we note that the sensitivity of the thermometry can further be improved by combining motional narrowing with contrast agents that show a change in magnetization at temperatures of interest. For example, Gadolinium silicide contrast agents show a sharp change in magnetization at around 30 °C[25]. Using nanoparticles of gadolinium silicide or similar contrast agents could

allow utilizing both motional narrowing and the temperature dependence of magnetization for biological thermometry with a higher sensitivity.

Methods

SQUID Magnetometry

SQUID magnetometry was performed on a Quantum Design MPMS 3 with temperature sweeps from 5 °C to 85 °C and a field sweep from -0.3 T to 0.3 T. Colloidal suspension of iron-oxide nanoparticles (0.18 ml with a density of 5 mg/ml) was held using a liquid sample holder (QD 8505-013).

NMR measurements

NMR linewidth and T_2 measurements were performed using a Varian Unity/Inova system using a 14.1 T (600 MHz) field and a 5mm broadband probe. FID spectra were collected at different temperatures using a relaxation delay (d1) of 4 s, an acquisition time of 1s, a spectral width of 15000 Hz and with 4 signal averages. Shimming the magnetic field was not possible for samples with the superparamagnetic particles, and the shim conditions for pure water were used for samples with the particles. CPMG pulse sequence [26] was used for determination of T_2 with a pulse spacing of 100 μ s with all other acquisition parameters identical to the FID measurements.

Sample temperature in the NMR probe were calibrated using the spectra of ethylene glycol above 35° C and using methanol from 5° C to 35° C at specific temperature set points controlled by a FTS temperature control system.

Linewidth and T_2 values were determined after data processing in Mnova.

MRI measurements

MRI measurements were performed using a Bruker BioSpec 9.4 T preclinical MRI system using an 80 mm volume coil. Isothermal T_2 and T_2^* measurements were performed on a 3 mm coronal slice (along the cross section of a cylindrical sample holder) with a slice size of 1 cm x 1 cm and a voxel size of 1 mm x 1 mm (x 3mm). T_2 mapping was obtained using a multispin multisecho (MSME) sequence [23] with an echo spacing of 5.6 ms and a total of 12 echo images. T_2^* mapping was performed using multi-gradient echo T_2^* map sequence with gradient echo spacing of 5.6 ms. A relaxation delay of 1 s was used for all acquisition. A signal averaging of four T_2 mapping resulted in a total acquisition time of 2 minutes and 13 s while four signal averaging for T_2^* mapping required a total of 2 minutes 0 s.

Isothermal heating of the samples was performed using a water pillow with heated water supplied using a Thermo Scientific Precision water bath. The isothermal condition of a MR slice was confirmed using two T-type thermocouples adjacent to the slice.

Image intensity analysis for T_2 and T_2^* mapping, as well as measurement of average variation in T_2 and T_2^* , were performed using Matlab.

Acknowledgements

The authors thank Dr. Shreyan Majumdar of the Beckman Imaging Center, University of Illinois for assistance with the MRI measurements and Dr. Lingyang Zhu of the School of Chemical Sciences, University of Illinois for assistance with the NMR measurements. This research was funded by Semiconductor Research Corporation (Task ID: 3044.0001).

References

- [1] V. Rieke and K. B. Pauly, "MR thermometry," *J. Magn. Reson. Imaging*, vol. 27, no. 2, pp. 376–390, 2008.
- [2] C. Stefanadis *et al.*, "Thermal heterogeneity constitutes a marker for the detection of malignant gastric lesions in vivo," *J. Clin. Gastroenterol.*, vol. 36, no. 3, pp. 215–218, 2003.
- [3] D. Bihan, J. Delaunoy, and R. Levin, "Temperature mapping with MR Imaging of molecular diffusion : Application to Hyperthermia," *Ther. Radiol.*, vol. 171, 1989.
- [4] F. Bertsch *et al.*, "Non-invasive temperature mapping using MRI: Comparison of two methods based on chemical shift and T1-relaxation," *Magn. Reson. Imaging*, vol. 16, no. 4, pp. 393–403, 1998.
- [5] Y. Ishihara *et al.*, "A precise and fast temperature mapping using water proton chemical shift," *Magn. Reson. Med.*, vol. 34, no. 6, pp. 814–823, 1995.
- [6] M. Holz, S. R. Heil, and A. Sacco, "Temperature-dependent self-diffusion coefficients of water and six selected molecular liquids for calibration in accurate 1H NMR PFG measurements," *Phys. Chem. Chem. Phys.*, vol. 2, no. 20, pp. 4740–4742, 2000.
- [7] D. C. Chang, H. E. Rorschach, B. L. Nicholls, and C. F. Hazlewood, "Implications of Diffusion Coefficient Measurements for the structure of cellular water," *Ann. New York Acad. Sci.*, vol. 204, pp. 434–43, 1973.
- [8] J. G. Li, G. J. Stanisiz, and R. M. Henkelman, "Integrated Analysis of Diffusion and Relaxation of Water in Blood," *Magn. Reson. Med.*, vol. 40, pp. 79–88, 1998.
- [9] I. Åslund and D. Topgaard, "Determination of the self-diffusion coefficient of intracellular water using PGSE NMR with variable gradient pulse length," *J. Magn. Reson.*, vol. 201, no. 2, pp. 250–254, 2009.
- [10] I. R. Jeon, J. G. Park, C. R. Haney, and T. D. Harris, "Spin crossover iron(ii) complexes as PARACEST MRI thermometers," *Chem. Sci.*, vol. 5, no. 6, pp. 2461–2465, 2014.
- [11] J. H. Hankiewicz, Z. Celinski, K. F. Stupic, N. R. Anderson, and R. E. Camley, "Ferromagnetic particles as magnetic resonance imaging temperature sensors," *Nat.*

- Commun.*, vol. 7, no. May, pp. 1–8, 2016.
- [12] S. Laurent *et al.*, “Magnetic iron oxide nanoparticles: Synthesis, stabilization, vectorization, physicochemical characterizations and biological applications,” *Chem. Rev.*, vol. 108, no. 6, pp. 2064–2110, 2008.
- [13] Wahajuddin and S. Arora, “Superparamagnetic iron oxide nanoparticles: Magnetic nanoplatforms as drug carriers,” *Int. J. Nanomedicine*, vol. 7, pp. 3445–3471, 2012.
- [14] Y.-X. J. Wang, S. M. Hussain, and G. P. Krestin, “Superparamagnetic iron oxide contrast agents: physicochemical characteristics and applications in MR imaging,” *Eur. Radiol.*, vol. 11, pp. 2319–2331, 2001.
- [15] B. Gleich and J. Weizenecker, “Tomographic imaging using the nonlinear response of magnetic particles,” *Nature*, vol. 435, no. 7046, pp. 1214–1217, 2005.
- [16] M. Gueron, “Nuclear relaxation in macromolecules by paramagnetic ions: a novel mechanism,” *J. Magn. Reson.*, vol. 19, no. 1, pp. 58–66, 1975.
- [17] R. Van Roosbroeck *et al.*, “Synthetic antiferromagnetic nanoparticles as potential contrast agents in MRI,” *ACS Nano*, vol. 8, no. 3, pp. 2269–2278, 2014.
- [18] S. Tong, S. Hou, Z. Zheng, J. Zhou, and G. Bao, “Coating optimization of superparamagnetic iron oxide nanoparticles for high T2 relaxivity,” *Nano Lett.*, vol. 10, no. 11, pp. 4607–4613, 2010.
- [19] R. Brooks, F. Moiny, and P. Gillis, “On T2-shortening by Weakly Magnetized Particles: The Chemical Exchange Model,” *Magn. Reson. Imaging*, vol. 45, no. 1014–1020, 2001.
- [20] J. M. Poller *et al.*, “Selection of potential iron oxide nanoparticles for breast cancer treatment based on in vitro cytotoxicity and cellular uptake,” *Int. J. Nanomedicine*, vol. 12, pp. 3207–3220, 2017.
- [21] J. Qin *et al.*, “A high-performance magnetic resonance imaging T2 contrast agent,” *Adv. Mater.*, vol. 19, no. 14, pp. 1874–1878, 2007.
- [22] K. Fabian, V. P. Shcherbakov, and S. A. McEnroe, “Measuring the Curie temperature,” *Geochemistry, Geophys. Geosystems*, vol. 14, no. 4, pp. 947–961, 2013.
- [23] Y. Fatemi, H. Danyali, M. S. Helfroush, and H. Amiri, “Fast T2 mapping using multi-echo spin-echo MRI: A linear order approach,” *Magn. Reson. Med.*, vol. 84, no. 5, pp. 2815–2830, 2020.
- [24] G. J. Stanisz *et al.*, “T1, T2 relaxation and magnetization transfer in tissue at 3T,” *Magn. Reson. Med.*, vol. 54, no. 3, pp. 507–512, 2005.
- [25] M. Nauman, M. H. Alnasir, M. A. Hamayun, Y. Wang, M. Shatruk, and S. Manzoor, “Size-dependent magnetic and magnetothermal properties of gadolinium silicide nanoparticles,” *RSC Adv.*, vol. 10, no. 47, pp. 28383–28389, 2020.
- [26] H. Y. Carr and E. M. Purcell, “Effects of diffusion on free precession in nuclear magnetic

resonance experiments," *Phys. Rev.*, vol. 94, no. 3, pp. 630–638, 1954.